J|A|C|S
COMMUNICATIONS

Published on Web 11/18/2006

Crystalline Graphite from an Organometallic Solution-Phase Reaction

Erich C. Walter,[†] Tobias Beetz,[‡] Matthew Y. Sfeir,[§] Louis E. Brus,[†] and Michael L. Steigerwald*,[†]

Department of Chemistry, Columbia University, 3000 Broadway Avenue, New York, New York 10027, and Center for Functional Nanomaterials and Condensed Matter Physics and Materials Science, Brookhaven National Laboratory, Upton, New York 11973

Received September 13, 2006; E-mail: mls2064@columbia.edu

Deposition of graphitic carbon via the catalytic decomposition and subsequent reconstitution of hydrocarbons is a very well studied process. Impact of this process has ranged from its deleterious effects in the carbonization of hydrocarbon reactors[1] to the remarkable science of single-walled carbon nanotubes, SWCNTs.[2] In general, the production of graphitic carbon in this way has required high reaction temperatures (500−1000 °C) or otherwise forcing chemical reaction conditions.[3−17] A more controllable process for the preparation of graphitic carbon (particularly graphene sheets and SWCNTs) would facilitate progress in these research areas by enabling the rational synthesis of desired forms of carbon. Here we report our observation that graphitic carbon, sheets as well as tubes, can be prepared from solution at temperatures as low as 110 °C.

During the effort to extend our previously reported[18] low-temperature preparation of nanocrystals of TiO_2, we have discovered that the reaction of $Fe(COT)_2$[19] with DMSO gives not only nanocrystals of iron oxides but also graphitic carbon (eq 1). $Fe(COT)_2$, dimethoxyethane (DME), and DMSO are combined in toluene, and the resulting mixture is heated to reflux for 5 days. A black precipitate forms, and when dried, the powder shows millimeter-sized fragments of a reflective black solid. Scanning electron microscopy (SEM) shows this to contain large amounts of long, tubular structures (Figure 1a).

Energy dispersive spectroscopy (EDS) shows primarily carbon with smaller amounts of iron and oxygen. Transmission electron microscopy (TEM) also shows sheets and micrometer long tubes, 4 nm in diameter (Figure 1b), in addition to nanoparticles of magnetite. The selective area electron diffraction (SAED) pattern in Figure 1B (inset) shows that the sheet/tube structures are crystalline, and the pattern matches that of crystalline graphite.[20] We observe only very weak [002] diffraction. We believe this indicates the paucity of stacked graphite sheets. When we soak[21] the black solid product of eq 1 in 0.37% HCl we find (Figure 2) that the FeO_x particles have been removed and that sheets and tubes of graphite remain. SAED confirms this identification.

$$Fe(COT)_2 + DMSO + DME \rightarrow Fe_3O_4 + \text{graphite} \quad (1)$$

We examined the product of eq 1 with high-resolution transmission electron microscopy (HRTEM) both before and after the material was treated with acid. The as-prepared sample was dominated by areas of crystalline graphite and multiwalled carbon nanotubes (MWCNTs). In Figure 3a we show a single graphitic tube. Measurement of the lattice spacing in all HTREM images having visible crystalline planes is ∼3.4 Å. This matches the interplanar distance for graphite.[22] The SAED pattern (Figure 3 inset) confirms this. Long-term exposure to the concentrated acid and sonication damages the graphite structure; in the HRTEM samples of this material we see no diffraction and no crystalline lattice, although we do observe tubular carbon structures (see Supporting Information).

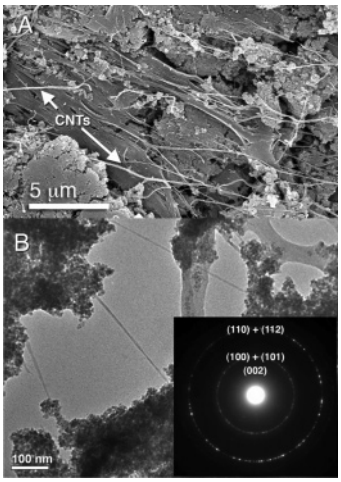

Figure 1. Electron microscopy of the initial product of eq 1: (A) SEM image of carbon nanotube bundles and FeO_x nanoparticles sputter-coated with a layer of Pd/Au for imaging; (B) TEM image showing sheets and tubes of carbon coated with the FeO_x nanoparticles; (inset) SAED pattern of an area dominated by graphitic sheets. The rings all match with literature values for graphite[20]

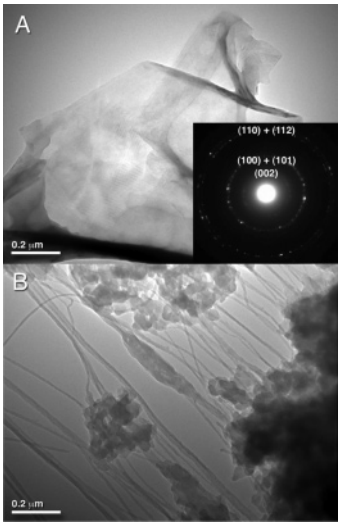

Figure 2. Effect of treatment with 0.37% HCl on eq 1. (A) TEM image showing that carbon sheets remain after the acid-treatment; the FeO_x nanoparticles are gone. Inset SAED pattern confirms the assignment as graphite; the (004) and (103) are present and very weak. Panel B shows the TEM image of carbon nanotubes that remain after the FeO_x nanoparticles are dissolved by concentrated HCl.

Raman spectroscopy is particularly useful in the identification of graphite and carbon nanotubes.[23−25] In Figure 4 we show the

[†] Columbia University.
[‡] Center for Functional Nanomaterials, Brookhaven National Laboratory.
[§] Condensed Matter Physics and Materials Science, Brookhaven National Laboratory.

10.1021/ja0666203 CCC: $33.50

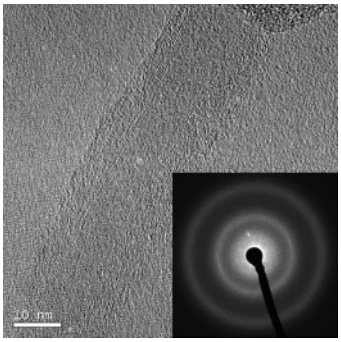

Figure 3. HRTEM analysis of the carbonaceous products of eq 1; HRTEM image of a MWCNT on a carbon film TEM grid. The measured distance between the parallel graphite planes is ~3.4 Å and agrees with the literature values for nanotubes and graphite. Inset is the SAED pattern. The pattern as well as the measured lattice spacings are consistent with data reported in the literature for CNTs. The diffuse rings are due to the amorphous carbon film support. The elongated diffraction spots at 2.05 Å arise from the nanotube structure.

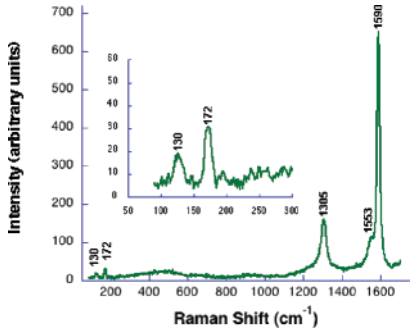

Figure 4. Raman Spectrum of the carbon product from eq 1. Present are the G-mode (1590 cm^{-1}) and D-mode (1305 cm^{-1}) peaks of graphite and possible radial breathing mode (130 and 172 cm^{-1}) peaks of carbon nanotubes. This spectrum is characteristic of crystalline graphite with some defects.

Raman spectrum of the black solid which had not been treated with acid excited by a helium-neon laser (632.8 nm). We observe the D (~1305 cm^{-1}) and G (~1590 cm^{-1}) modes of crystalline graphite. The peaks at 130 cm^{-1} and 172 cm^{-1} are intriguing; they may be attributed to radial breathing modes of CNTs.[26] The Raman spectrum also shows that treating the product with acid damages the graphitic carbon: acid-treated samples display weak, broad peaks at 1350 cm^{-1} and around 1590 cm^{-1}.

We have yet to characterize completely this process, but several aspects are worth noting. The process is slow; we do not observe a significant amount of graphitic carbon after just 12 h at reflux. At higher temperatures (300 °C in heptadecane) we do see graphite after just 16 h. The process is not simply the pyrolysis of $Fe(COT)_2$—when $Fe(COT)_2$ is heated in toluene at reflux in the absence of DMSO we do not observe graphite. The process is not uniquely a property of $Fe(COT)_2$—the reaction of COT with $Fe(CO)_5$ in the presence of 5 mol equiv of trimethylamine *N*-oxide[27] in refluxing toluene also produces graphitic carbon after 5 days. It is unclear whether an ancillary ligand such as DME is required—when DMSO and $Fe(COT)_2$ are heated in the absence of DME, graphite is also produced. It is clear that Fe (or some other catalytic agent) is required; no graphite results when COT is heated with DMSO in toluene.

The formation of crystalline graphite under such mild conditions is unprecedented. It is not yet clear which form of Fe is responsible for the formation of graphite. While we can be certain that FeO_x nanoparticles are formed, we cannot be certain that it is they that catalyze the apparent dehydrogenation/polymerization of COT. However, we do observe carbon as a product of the reaction COT and DMSO in refluxing toluene in the presence of independently prepared, commercially available, nanometer-scale particles of either Fe_2O_3 or Fe_3O_4. The growth of carbon nanotubes is achieved almost exclusively by metal−nanoparticle catalysis under CVD conditions at high temperatures (400−1000 °C); therefore, it is reasonable to propose that the FeO_x nanoparticles are catalytically active.

This work introduces a new method for the catalytic preparation of several forms of crystalline graphite. At present the reaction is not selective with respect to which form of graphite is produced; however, since the entire process occurs at low temperatures, we anticipate being able to kinetically control and direct it once we fully characterize the catalytic centers.[28]

Acknowledgment. This work has been primarily supported at Columbia by the NSF via the MRSEC program (Grant DMR-0213574), by the Nanoscale Science and Engineering Initiative of the National Science Foundation under NSF Award Number CHE-0117752, and by the New York State Office of Science, Technology, and Academic Research (NYSTAR). We gratefully acknowledge the assistance of a reviewer who indicated an error in interpretation in our original manuscript.

Supporting Information Available: Experimental details and additional TEM images including an expanded Figure 2 inset. This material is available free of charge via the Internet at http://pubs.acs.org.

References

(1) Tan, C. D.; Baker, R. T. K. *Catal. Today* **2000**, *63*, 3.
(2) Satio, R.; Dresselhaus, G. D.; Dresselhaus, M. S. *Physical Properties of Carbon Nanotubes*; Imperial College Press: London, 1998.
(3) Govindaraj, A.; Rao, C. N. R. *Pure Appl. Chem.* **2002**, *74*, 1571.
(4) Hwang, H. J.; Kajiura, H.; Tsutsui, S.; Hirano, Y.; Miyakoshi, M.; Yamada, A.; Ata, M. *Chem. Phys. Lett.* **2002**, *343*, 7.
(5) Hu, J.; Bando, Y.; Zhan, J.; Zhi, C.; Xu, F.; Golberg, D. *Adv. Mater.* **2006**, *18*, 197.
(6) Harris, J. D.; Raffaelle, R. P.; Gennett, T.; Landi, B. J.; Hepp, A. F. *Mater. Sci. Eng., B* **2005**, *116*, 369.
(7) O'Loughlin, J. L.; Kiang, C. H.; Wallace, C. H.; Reynolds, T. K.; Rao, L.; Kaner, R. B. *J. Phys. Chem. B* **2001**, *105*, 1921.
(8) Zhi, L.; Wu, J.; Li, J; Kolb, U; Müllen, K. *Angew. Chem., Int. Ed.* **2005**, *44*, 2120.
(9) Laskoski, M.; Steffen, W.; Morton, J. G. M.; Smith, M. D.; Bunz, U. H. F. *J. Am. Chem. Soc.* **2002**, *124*, 13814.
(10) Mohlala, M. S.; Liu, X.-Y.; Robinson, J. M.; Coville, N. J. *Organometallics* **2005**, *24*, 972.
(11) Zhou, O.; Shimoda, H.; Gao, B.; Oh, S.; Fleming, L.; Yue, G. *Acc. Chem. Res.* **2002**, *35*, 1045.
(12) Vander Wal, R. L.; Ticich, T. M.; Curtis, V. E. *Chem. Phys. Lett.* **2000**, *323*, 217.
(13) Bandow, S.; Asaka, S.; Saito, Y.; Rao, A. M.; Grigorian, L.; Richter, E.; Eklund, P. C. *Phys. Rev. Lett.* **1998**, *80*, 3779.
(14) Iyer Vivekanantan, S.; Volhardt, K. P. C.; Wilhelm, R. *Angew. Chem., Int. Ed.* **2003**, *42*, 4379.
(15) Wang, S.; Wang, P.; Zhou, O. *Diamond Relat. Mater.* **2006**, *15*, 361.
(16) Keller, T. M.; Qadrib, S. B.; Little, C. A. *J. Mater. Chem.* **2004**, *14*, 3063.
(17) Ajaman, P. M. *Chem. Rev.* **1999**, *99*, 1787.
(18) Tang, J.; Redl, F.; Zhu, Y.; Siegrist, T.; Brus, L. E.; Steigerwald, M. L. *Nano Lett.* **2005**, *5*, 543.
(19) Gerlach, D. H.; Schunn, R. A. *Inorg. Synth.* **1974**, *15*, 2.
(20) Wang, J. J.; Zhu, M. Y.; Outlaw, R. A.; Zhao, X.; Manos, D. M.; Holloway, B. C. *Appl. Phys. Lett.* **2004**, *85*, 1265.
(21) Vivekchand, S. R. C.; Jayakanth, R.; Govindaraj, A.; Rao, C. N. R. *Small* **2005**, *1*, 920.
(22) Mark, H.; Hassel, O. *Z. Phys.* **1924**, *25*, 317−337.
(23) Ferrari, A. C.; Robertson, J. *Phys. Rev. B: Condens. Matter Mater. Phys.* **2000**, *61*, 14095−14107.
(24) Tuinstra, F.; Koenig, J. L. *J. Chem. Phys.* **1970**, *53*, 1126.
(25) Dresselhaus, M. S.; Dresselhaus, G.; Jorio, A.; Souza Filho, A. G.; Pimenta, M. A.; Satio, R. *Acc. Chem. Res.* **2002**, *35*, 1070.
(26) Rao, A. M.; Richter, E.; Bandow, S.; Chase, B.; Eklund, P. C.; Williams, K. A.; Fang, S.; Subbaswamy, K. R.; Menon, M; Thess, A; Smalley, R. E.; Dresselhaus, G.; Dresselhaus, M. S. *Science* **1997**, *275*, 187.
(27) Albers, M. O.; Coville, N. J. *Coord. Chem. Rev.* **1984**, *53*, 227.
(28) Rodriguez, N. M.; Chambers, A.; Baker, R. T. K. *Langmuir* **1995**, *11*, 3862.

JA0666203